A Bosonic Model of Hole Pairs

Thomas Siller [1], Matthias Troyer[1], T. M. Rice[1], Steven R. White[2]

1 *Theoretische Physik, Eidgenössische Technische Hochschule, CH-8093 Zürich, Switzerland*
2 *Department of Physics and Astronomy, University of California Irvine, CA 92697*

(February 1, 2008)

We numerically investigate a bosonic representation for hole pairs on a two-leg t-J ladder where hard core bosons on a chain represent the hole pairs on the ladder. The interaction between hole pairs is obtained by fitting the density profile obtained with the effective model to the one obtained with the t-J model, taking into account the inner structure of the hole pair given by the hole-hole correlation function. For these interactions we calculate the Luttinger liquid parameter, which takes the universal value $K_\rho = 1$ as half filling is approached, for values of the rung exchange J' between strong coupling and the isotropic case. The long distance behavior of the hole-hole correlation function is also investigated. Starting from large J', the correlation length first increases as expected, but diminishes significantly as J' is reduced and bound holes sit mainly on adjacent rungs. As the isotropic case is approached, the correlation length increases again. This effect is related to the different kind of bonds in the region between the two holes of a hole pair when they move apart.

I. INTRODUCTION

The study of strongly correlated electrons in ladder systems has been an active field in recent years. Ladders consisting of a number of coupled legs (or chains) show a rich variety of phases [1–6] depending on the number of legs and the electron density. One property of particular interest is the binding of holes into pairs when weakly doped into a half-filled two leg ladder, to form a Luther-Emery liquid. In this liquid the spin degrees of freedom are gapped and the low energy sector can be mapped to a boson liquid of hole pairs. This can be studied analytically in the weak coupling limit described, for example, by a one-band Hubbard model with weak interactions. In the strongly interacting limit described by a t-J model, [7] one must use numerical methods such as Lanczos diagonalization and the recently developed Density Matrix Renormalization Group (DMRG) method. [8,9] Large simulations can be carried out using the DMRG yielding information on the equal time correlations.

In this paper our goal is to use the hole density distributions determined by DMRG to determine the form of the effective boson model that we know on general grounds describes the hole pairs. We use these DMRG results to parameterize their dispersion and their effective mutual interactions and also the interaction with hard wall boundary conditions that occur in DMRG. In this first paper we limit ourselves to the simplest case of the two leg ladder. The same approach can be made for wider ladders with an even number of legs and is currently in progress.

We start with the t-J ladder Hamiltonian

$$H = -t \sum_{i,j,\sigma} \mathcal{P}(c^\dagger_{i,j,\sigma} c_{i+1,j,\sigma} + c^\dagger_{i+1,j,\sigma} c_{i,j,\sigma}) \mathcal{P} \qquad (1)$$

$$-t' \sum_{i,\sigma} \mathcal{P}(c^\dagger_{i,1,\sigma} c_{i,2,\sigma} + c^\dagger_{i,2,\sigma} c_{i,1,\sigma}) \mathcal{P}$$

$$+J \sum_{i,j} (\mathbf{S}_{i,j} \mathbf{S}_{i+1,j} - \frac{1}{4} n_{i,j} n_{i+1,j})$$

$$+J' \sum_i (\mathbf{S}_{i,1} \mathbf{S}_{i,2} - \frac{1}{4} n_{i,1} n_{i,2})$$

where i runs over L rungs, $j(= 1, 2)$ and σ $(=\uparrow, \downarrow)$ are leg and spin indices. The projection operator $\mathcal{P} \equiv \prod_{i,j}(1 - n_{i,j,\uparrow} n_{i,j,\downarrow})$ prohibits double occupancy of a site. Unless noted otherwise we set $t = t'$ and $J = 0.35\,t$.

II. THE STRUCTURE OF A HOLE PAIR

In this section we examine a hole pair on a t-J ladder, studying the internal hole-hole correlation (hhc) function. The hhc function gives us information about the inner structure of a hole pair and depends on the parameters t, t', J and J' in the t-J Hamiltonian given above. Since the DMRG computations are performed with open boundaries, special care must be taken in the measurement of the hhc-function, which we define as

$$g_j(r_1, r_2) = \frac{\langle n^h_{r_1,1} n^h_{r_2,j} \rangle}{\langle n^h_{r_1,1} \rangle \langle n^h_{r_2,j} \rangle} n^h . \qquad (2)$$

The index $j = 1, 2$ denotes intra- and inter-leg-correlations respectively, $n^h_{i,j} = 1 - n_{i,j}$ denotes the hole density at site (i, j), and n^h the average hole density. Introducing relative and center of mass coordinates, r and R_0, we measure $g_j(r, R_0)$ on (40×2)-ladders with open boundaries for $R_0 \simeq L/2$. In a range $R_0 = L/2 \pm 5$, $g_j(r, R_0)$ depends only weakly on R_0. Furthermore, we have tested that better accuracy for the hhc-function cannot be achieved on larger ladders up to (60×2) sites. We conclude that these measurements give good values for $g_j(r)$ on an infinite ladder.

We denote by

$$g(r) = \sum_j g_j(r) \qquad (3)$$

the sum of intra- and inter-leg correlations. We have examined $g(r)$ as a function of the rung exchange coupling J'. As can be seen in Fig. 1, a significant change in the hhc-function occurs when the isotropic case ($J' \to J$) is approached from the strong rung coupling regime ($J' \gg J$). In the latter case, the holes sit mainly on the same rung whereas in the former case, they are found predominantly on adjacent rungs. We study the long distance behavior of the hhc-function by fitting the tail to an exponentially decaying function, $g(r) \sim \exp(-r/\xi_{hhc})$. The results are shown in Fig. 2, where ξ_{hhc} is plotted as a function of J'. Starting from strong rung coupling, the correlation length first increases as expected, but decreases significantly as J' is reduced and bound holes sit mainly on adjacent rungs. As the isotropic case is approached, the correlation length increases again.

This behavior can be explained by looking at the different kinds of bonds in the region between two holes of a pair as the holes move apart. In Fig. 3, we show the exchange fields around a pair of holes. These are obtained by measuring $\mathbf{S}_i \cdot \mathbf{S}_j$ after projecting out a particular configuration of two holes from the ground state $|\psi\rangle$ given for two holes on a (16×2)-ladder. Denoting the corresponding projection operator by P_h, $P_h \mathbf{S}_i \cdot \mathbf{S}_j P_h$ has been measured and normalized by $\langle\psi|P_h|\psi\rangle$. The procedure is well described by White and Scalapino. [10] This kind of measurement gives us a "snapshot" of the spin configuration around a dynamic hole. In the following we use the term "bond" simply to indicate that $\langle \mathbf{S}_i \cdot \mathbf{S}_j \rangle < 0$. If this expectation value is close to -0.75 for two sites i and j, we say that there is a "singlet bond" connecting i and j.

For $J' > 1.2\,t$ the rung exchange dominates. When a hole pair virtually splits up, the region between the two holes reverts to rung singlets, as shown in Fig. 3. A high energy is needed to split up the holes, but after they are separated there is no further increase in energy in moving them apart, since the diagonal exchange bonds are weak. For $J' < 0.7\,t$ the region between the holes does something more complicated, which facilitates hole hopping at the expense of higher exchange energy on the intervening rungs. As shown in Fig. 3, various diagonal exchange bonds are formed, which turn into the rung singlets when the holes hop back together. This allows for easy hopping and low kinetic energy, but the exchange energy cost is high. For $J' = 0.7\,t$, more and more distorted exchange bonds are created as the holes move apart. This leads to a stronger interaction for larger separation than in the case for $J' = 1.2\,t$. This weakening of the long range interaction between the two holes explains the increase of ξ_{hhc} in Fig. 2 in the range between $J' = 0.7\,t$ and $J' \simeq 1.2\,t$.

Somewhat similar analysis can be found in Ref. [10] where the authors have argued that the exchange bonds seen in Fig. 3 are responsible for the pairing seen in the isotropic case, as well as for stripe formation.

III. THE EFFECTIVE MODEL FOR HOLE PAIRS

In the strong coupling limit $J' \gg J$, in the ground state, two bound holes are on the same rung and a description of tightly bound hole pairs moving in a background of singlet rungs is appropriate. Considering these hole pairs as hard core bosons (hcb) one can map to an effective boson model as discussed in Ref. [5] and obtain the hole density directly from the corresponding hcb density as well as the correlations between hole pairs.

Here we propose an effective model that applies for any value of J' between strong coupling and the isotropic case. Since holes on a ladder can pair with more weight on adjacent rungs, our effective model should incorporate the possibility that the "center of mass" of a hole pair can lie on a rung or between two rungs as shown in Fig. 4. Note that for even (odd) distance r along the legs between two holes, the center of mass lies on a rung (between two rungs).

To motivate our effective model we study first the case of pairing between two holes on a two-leg ladder with length L where the Hamiltonian is given by

$$H = -t_h \sum_{j=1}^{2} \sum_{i=1}^{L} (b_{i,j}^\dagger b_{i+1,j} + b_{i+1,j}^\dagger b_{i,j}) \qquad (4)$$
$$-t_h \sum_{i=1}^{L} (b_{i,1}^\dagger b_{i,2} + b_{i,2}^\dagger b_{i,1}) + V_h \quad .$$

Here $b_i^\dagger$ and b_i denote hole creation and annihilation operators respectively. Only single occupation of a site is allowed and we use periodic boundary conditions. We choose the attractive interaction V_h between the two holes strong enough to give an even parity bound state. We want to find an effective Hamiltonian for the paired holes, expressed in terms of a new effective boson operator $B_i^\dagger$ which describes the pair as a whole, and then answer the question, how do we obtain the hole density $n_{i,j}^b = b_{i,j}^\dagger b_{i,j}$ from the density $N_i = B_i^\dagger B_i$ of the effective bosons?

For the Hamiltonian above, with the help of the operators

$$p_{R,r}^\dagger = \frac{1}{\sqrt{2}} (b_{R-\frac{r}{2},1}^\dagger b_{R+\frac{r}{2},1}^\dagger + b_{R-\frac{r}{2},2}^\dagger b_{R+\frac{r}{2},2}^\dagger)(1 - \delta_{r,0}) \quad (5)$$

$$\tilde{p}_{R,r}^\dagger = \begin{cases} \frac{1}{\sqrt{2}} (b_{R-\frac{r}{2},1}^\dagger b_{R+\frac{r}{2},2}^\dagger + b_{R-\frac{r}{2},2}^\dagger b_{R+\frac{r}{2},1}^\dagger) & r \neq 0 \\ b_{R-\frac{r}{2},1}^\dagger b_{R+\frac{r}{2},2}^\dagger & r = 0 \end{cases} \quad (6)$$

the wavefunction $\Psi^\dagger|0\rangle$ for the ground state can be written as

$$\Psi^\dagger = \frac{1}{\sqrt{L}} \sum_{R=\text{int.}} \sum_{r_{\text{even}}} \left(\varphi_1(r)\, p_{R,r}^\dagger + \varphi_2(r)\, \tilde{p}_{R,r}^\dagger\right) \qquad (7)$$
$$+ \frac{1}{\sqrt{L}} \sum_{R=\text{half}} \sum_{r_{\text{odd}}} \left(\varphi_1(r)\, p_{R,r}^\dagger + \varphi_2(r)\, \tilde{p}_{R,r}^\dagger\right) \quad .$$

Here R and $r(= 0, 1, 2, \ldots)$ denote the center of mass and relative coordinates along the legs as sketched in Fig. 4. $\varphi_j(r)$ depends only on r and the interaction V_h in Eq. (4). The pair correlation function $g_j(r)$ for the holes $b_i^\dagger$ in this model is simply given by $g_j(r) = |\varphi_j(r)|^2$, where $j = 1, 2$ denote intra- and inter-leg correlations respectively.

The probability of finding the center of mass of a pair centered on a rung, w_{int}, or between two rungs, w_{half}, is given by

$$w_{\text{int}} = \sum_{r_{\text{even}}} |\varphi_1(r)|^2 + |\varphi_2(r)|^2 = \sum_{r_{\text{even}}} g(r) \quad (8)$$

$$w_{\text{half}} = \sum_{r_{\text{odd}}} |\varphi_1(r)|^2 + |\varphi_2(r)|^2 = \sum_{r_{\text{odd}}} g(r)$$

where $g(r)$ denotes the sum of the inter- and intra-leg correlations as defined in Eq. (3). Note that the probability to find the pair on or between rungs depends only on whether R is integer or half integer.

The same occupation probabilities can be obtained with the Hamiltonian

$$H = -t^* \sum_{R=\frac{1}{2}, 1, \ldots}^{L} (B_R^\dagger B_{R+\frac{1}{2}} + B_{R+\frac{1}{2}}^\dagger B_R) + \epsilon \sum_{R=\frac{1}{2}, \frac{3}{2}, \ldots}^{L+\frac{1}{2}} N_R \quad (9)$$

for one boson $B_R^\dagger$ which moves on a closed chain of length L under the action of a periodically varying onsite potential ϵ. Here $N_R = B_R^\dagger B_R$.

Figure 4 shows the mapping of hole pairs from the ladder to effective bosons on a single chain. Note that the center of mass coordinate R of the pairs determines the position of the effective boson. Here the ratio of the probabilities $w_{\text{half}}/w_{\text{int}}$ to find the boson on a site with half integer or integer R depends only on ϵ/t^* and can easily be obtained as

$$\frac{w_{\text{half}}}{w_{\text{int}}} = \frac{\epsilon^2 + (4t^*)^2 - \epsilon\sqrt{\epsilon^2 + (4t^*)^2}}{\epsilon^2 + (4t^*)^2 + \epsilon\sqrt{\epsilon^2 + (4t^*)^2}} \ . \quad (10)$$

From this equation and Eq. (8) we obtain for ϵ

$$\epsilon = 4\, t^* \sinh\left(\ln\left|\sqrt{\frac{\sum_{r_{\text{even}}} g(r)}{\sum_{r_{\text{odd}}} g(r)}}\right|\right) \ . \quad (11)$$

The boson operator $B_R^\dagger$ can be expressed in terms of the operators $p_{R,r}^\dagger$ and $\tilde{p}_{R,r}^\dagger$ as

$$B_R^\dagger = \begin{cases} \dfrac{\sum_{r_{\text{even}}} \left(\varphi_1(r)\, p_{R,r}^\dagger + \varphi_2(r)\, \tilde{p}_{R,r}^\dagger\right)}{\left[\sum_{r_{\text{even}}} g(r)\right]^{\frac{1}{2}}} & \text{for int. } R \\[4mm] \dfrac{\sum_{r_{\text{odd}}} \left(\varphi_1(r)\, p_{R,r}^\dagger + \varphi_2(r)\, \tilde{p}_{R,r}^\dagger\right)}{\left[\sum_{r_{\text{odd}}} g(r)\right]^{\frac{1}{2}}} & \text{for half int. } R \end{cases} \quad (12)$$

Once the density N_R for the model (9) has been computed, we obtain the density $n_{i,j}^b = b_{i,j}^\dagger b_{i,j}$ for the model

(4), taking into account the inner structure of the effective boson (12) by the convolution

$$n_{i,j}^b = \frac{1}{2} \frac{\sum_{r_{\text{even}}} g(r)(N_{i-\frac{r}{2}} + N_{i+\frac{r}{2}})}{\sum_{r_{\text{even}}} g(r)} \quad (13)$$
$$+ \frac{1}{2} \frac{\sum_{r_{\text{odd}}} g(r)(N_{i-\frac{r}{2}} + N_{i+\frac{r}{2}})}{\sum_{r_{\text{odd}}} g(r)} \ .$$

We are interested in the ground state properties of the t-J model. Since the spin part of the ground state wavefunction is antisymmetric and the spin excitations are gapped, [5] the charge degrees of freedom can be described considering hole pairs as effective (hard core) bosons moving in a spin liquid.

To obtain the effective Hamiltonian describing hole pairs in the t-J model (1), we model the holes as in Eq. (4) and define in analogy to the preceding

$$H = -t^* \sum_{R=1, \frac{1}{2}, \ldots}^{L-\frac{1}{2}} (B_R^\dagger B_{R+\frac{1}{2}} + B_{R+\frac{1}{2}}^\dagger B_R) \quad (14)$$
$$+ \epsilon \sum_{R=\frac{3}{2}, \frac{5}{2}, \ldots}^{L-\frac{1}{2}} N_R + V_{\text{int}} + V_b$$

where $N_R = B_R^\dagger B_R$ and the $B_R^\dagger$ and B_R denote hcb creation and destruction operators respectively. Since we are using open boundaries, we have to take into account the interaction of the hole-pairs with the boundaries. The potential V_b has been introduced to describe this effect. The potential V_{int} gives the interaction between hcb, i.e. hole pairs in the t-J model. The onsite potential ϵ on half-integer sites has the same meaning as explained above.

IV. COMPUTING THE MODEL PARAMETERS

In this section we determine the effective model parameters t^*, ϵ and the interactions V_b and V_{int}.

A. Onsite potential ϵ

The onsite potential ϵ has been calculated with the hhc-function $g(r)$ obtained numerically by the DMRG for two holes on (40×2) t-J ladders for various J'. The results are given in Fig. 5. They clearly show that for the isotropic case, i.e. $J = J'$, where $\epsilon < 0$, the hole pair is mainly centered between two rungs, whereas for strong coupling, i.e. $J' \gg J$, where $\epsilon > 0$, both holes of a pair sit on the same rung and can be well described by the effective model given in Ref. [5].

3

B. Interaction with the boundaries

As ϵ is determined by the hhc-function alone, we can compute the hcb density N_i, convolute it with $g(r)$ according to Eq. (13) and compare it with the hole density n_i^h of the corresponding t-J system. The hole density $n_{i,j}^h$ can be obtained using Eq. (13) by identifying $n_{i,j}^b$ with $n_{i,j}^h$. In this way we obtain V_b and V_{int} by fitting the density profile obtained with the effective model to the one obtained with the t-J model. Since V_{int} in Eq. (9) gives no contribution for one hcb, we can obtain V_b by considering one hole pair in the t-J model. We choose an exponentially decreasing form for V_b

$$V_b = v_b \sum_R N_R \left(e^{-\frac{R-1}{\xi_b}} + e^{-\frac{L-R}{\xi_b}} \right) \qquad (15)$$

with increasing distance from the boundary. Figure 6 shows fits for $J' = 0.35\,t$ and $J' = 10\,t$. and the parameters v_b and ξ_b are shown in Fig. 7. Up to $J' = 3.0\,t$, v_b is positive and ξ_b is finite. Above this value v_b becomes negative and ξ_b is zero. In this case only the outermost rungs become attractive for hole pairs as can be expected for large J', due to the charge part $-\frac{1}{4}\,n_{i,j}^h\,n_{i+1,j}^h$ of the J' term.

C. The interaction term V_{int}

To obtain the interaction potential V_{int} we proceed in the same way as for V_b. We choose a hard core analytical form

$$V_{\text{int}} = \sum_R \sum_{R'>R} v_{\text{int}}(|R - R'|)\, N_R N_{R'} \qquad (16)$$

$$v_{\text{int}}(r) = \begin{cases} \infty & \text{if } r < r_{min} \\ v_1 & r = r_{min} \\ v\,e^{-\frac{r-r_{min}-\frac{1}{2}}{\xi}} & \text{if } r > r_{min} \end{cases}$$

with $r_{min} \geq 1$ and considered (30×2) t-J ladders with four holes and the corresponding effective model with two hcb. The infinite repulsion for $r = \frac{1}{2}$ reflects the hard core condition for hole pairs, so that the minimum distance of two hole pairs in the t-J model is 1.

Since the hole pair becomes broader with decreasing J', it was useful to let r_{min} vary. Again, we have made fits between the density profiles as shown in Fig. 8 and obtained the parameters represented in Table I. Figure 9 shows v_{int} for different J' values. Starting from the isotropic case, the interaction is repulsive and becomes less long ranged as J' increases. For $J' = 5\,t$, v_{int} becomes negative for $r = 2$. The same holds for $J' = 10\,t$, where v_{int} vanishes for $r > 2$. This can be expected from a perturbative approach as can be found in Ref. [5], where the hole pairs on a t-J ladder have been mapped to hcb on a chain with next-nearest neighbor interaction.

We have tested the results obtained in this way by comparing the density profiles for various numbers of hole pairs and system lengths. From strong coupling down to the isotropic case we find good agreement between the density profiles obtained from the t-J model and the effective model, as can be seen in Fig. 10.

We should note here that the fits for v_{int} were not as stable as the fits for v_b. Varying simultaneously the parameters v_1, v and ξ in Eq. (15), one can find another set of parameters which also gives a good fit. However, we found that the Luttinger liquid parameter K_ρ, which we calculate in the next section, only weakly depends on this ambiguity. Using only two parameters to determine v_{int} suppressing v_1 in Eq. (15), one can also fit the density profiles with a different set of parameters, but in this case K_ρ is strongly affected.

D. The hopping matrix element t^*

Up to now the hopping matrix element t^* did not play any role. We were only interested in the hcb density profile, which is not affected by the energy scale fixed by t^*.

We compute t^* by finite size scaling with the ansatz that the difference between the ground state energy for two holes $E_{2\text{h}}$ and for zero holes $E_{0\text{h}}$ in the t-J model is given by

$$E_{2\text{h}}(L) - E_{0\text{h}}(L) \simeq \text{const} + t^* E_{\text{eff}}(L) . \qquad (17)$$

Here E_{eff} denotes the ground state energy of the corresponding effective model with one boson and with $t^* = 1$. We obtained t^* by fitting Eq. (17) to a straight line. The result is shown in Fig. 11.

According to the effective model given in Ref. [5], one can obtain the corresponding effective hopping matrix element t^o by a finite size scaling with the ansatz

$$E_{2\text{h}}(L) - E_{0\text{h}}(L) \simeq \text{const} + t^o(\pi/(L+1))^2 . \qquad (18)$$

Here, $E_{2\text{h}}(L)$ and $E_{0\text{h}}(L)$ are for the t-J model. A perturbative estimate for t^o is given in Ref. [5]. For large J' one obtains

$$t^o = 2\,t^2/(J' - 4\,t^2/J') . \qquad (19)$$

Figure 11 shows t^o versus J'. It can be seen that for $J' \to \infty$ the t^o obtained by perturbation theory tends to the one obtained by finite size scaling. Note that t^o stands for the hopping of a hole pair from one rung to another, whereas in our effective model t^* mediates between i and $i + \frac{1}{2}$. We can obtain t^o from t^* by expanding the single boson dispersion of the effective model for small momenta k. In this way we obtain

$$t^o = \frac{t^{*2}}{\sqrt{\epsilon^2 + (4\,t^*)^2}} . \qquad (20)$$

Figure 11 shows that t^o obtained in this way from our effective model fits very well to the one obtained by finite size scaling.

An independent test for t^* comes from the comparison of the inverse compressibility κ^{-1} obtained from the t-J model and the effective model. The inverse compressibility could be obtained from

$$\kappa^{-1}(\rho) = \frac{\rho^2}{\Omega} \frac{\partial^2 E_0(\rho)}{\partial \rho^2} \ . \tag{21}$$

Here the volume $\Omega = 2\,L$ for the t-J model and $\Omega = 2\,L - 1$ for the effective model. With N we denote the hole or hcb number and with $\rho = N/\Omega$ the corresponding density. The second derivative of the ground state energy with respect to the particle number N was calculated by the discretization

$$\frac{\partial^2 E_0}{\partial N^2} \simeq \frac{E_0(N+\Delta) - 2\,E_0(N) + E_0(N-\Delta)}{\Delta^2} \ . \tag{22}$$

Here $\Delta = 2$ and $\Delta = 1$ has been used for the t-J model and the effective model respectively. Figure 12 shows the results for κ^{-1} computed for a (40×2) t-J ladder with 2 holes and 4 holes. As can be expected, the results agree better for large J', where the hole pairs are narrower and the interaction between pairs is less long-ranged, but the agreement is satisfactory for all values of J'/t.

V. LUTTINGER LIQUID PARAMETER K_ρ

In the previous section we obtained the interaction between two hcb in the effective model (i.e. two hole pairs in the t-J model). In order to obtain information about the long range correlations we have calculated the Luttinger liquid parameter K_ρ in the effective model.

Our effective model belongs to the same universality class as the hcb model with next-nearest neighbor interaction, which in turn is equivalent to the XXZ model and which has been solved exactly by a bosonization approach and conformal field theory. [11,12] From Ref. [11] we obtain a power law decay at large distances for the charge density wave correlations and the superconducting correlations given as

$$\langle N_r N_0 \rangle \sim \text{const} \times r^{-2} + \text{const} \times \cos(2\pi\rho\,r)\,r^{-2\,K_\rho} \tag{23}$$

$$\langle B_r^\dagger B_0 \rangle \sim \text{const} \times r^{-\frac{1}{2\,K_\rho}} \ . \tag{24}$$

Here ρ denotes the electron density on the ladder and half filling corresponds to $\rho = 1$. These relations show that the superconducting correlations $\langle B_r^\dagger B_0 \rangle$ are dominant if $K_\rho > \frac{1}{2}$.

For hcb in one dimension, K_ρ can also be obtained from the relations [13]

$$K_\rho = \pi v_c L \left(\frac{\partial^2 E_0}{\partial N_b^2} \right)^{-1} \tag{25}$$

$$v_c K_\rho = \frac{\pi}{L} \left. \frac{\partial^2 E_0(\Phi)}{\partial \Phi^2} \right|_{\Phi=0} \ .$$

Here E_0 denotes the ground state energy for a closed ring of length L with N_b hcb and $E_0(\Phi)$ is the ground state energy of the system penetrated by a magnetic flux Φ which modifies the hopping by the usual Peierls phase factor, $t \mapsto t \exp(\pm i\Phi/L)$. From these two equations the charge velocity v_c can be eliminated. The second derivative of the ground state energy with respect to the particle number was calculated by the discretization given in Eq. (22) with $\Delta = 1$. We used exact diagonalization for system lengths between 32 and 220 and with N_b between 2 and 4. Analogously, the second derivative with respect to the magnetic flux was calculated for the same configurations.

We calculated the Luttinger liquid parameter K_ρ for the interaction potentials given by the parameters in Table I and found the universal value $K_\rho = 1$ as half filling is approached, for any value of J' between strong coupling and the isotropic case (Figs. 13 and 14). For $N_b/L \to 0$, corresponding to a very dilute hcb gas, we have $K_\rho = 1 + O(N_b/L)$, independent of the value of the interaction and consistent with Refs. [14,15]. Down to $\rho \simeq 0.875$ the superconducting correlations are dominant, since $K_\rho > \frac{1}{2}$ and since we are far away from phase separation. [5] Below $\rho \simeq 0.875$, K_ρ becomes less than one half and at one quarter doping ($\rho = 0.75$) $K_\rho < \frac{1}{2}$ for $J' \leq t$. Figure 13 shows also earlier results on small clusters from Ref. [5] and Ref. [16], obtained using exact diagonalization. The deviations from our results are most probably due to finite size effects close to half filling in Ref. [5] and Ref. [16].

We briefly want to discuss the possibility of commensurability effects. At a filling of $\rho = 0.75$, one might expect that commensurability effects would stabilize long ranged charge density wave ordering, since K_ρ is quite small ($K_\rho = 0.232$ for the isotropic case). In the finite, open systems studied here, a static CDW is pinned by the boundaries, as can be seen in Fig. 16 for the t-J model as well as in Fig. 15 for the effective model. A careful analysis using large systems and finite size scaling is necessary to determine if the CDW order is long ranged. The decay of CDW oscillations away from the edges of the system is quite slow and is consistent with long ranged CDW order, but a very slow algebraic decay cannot be ruled out. A more detailed analysis of the effective model (using 200, 240, 280, 320 and 400 sites) shows a decreasing charge gap with increasing system size. Finite size scaling is consistent with a vanishing or possibly a small charge gap in the infinite system.

VI. CONCLUSIONS

The effective model derived in this paper works well for the hole density of a two-leg t-J ladder for various fillings. In other words, the low energy physics of hole pairs on a ladder can be well described by a model of hard core bosons on a chain with each boson representing a pair of holes. The interaction between the hard core

bosons was determined by fitting the density profile obtained with the effective model to that of the t-J model, taking into account the inner structure of the hole pair given by the hole-hole correlation function. Starting from the isotropic case, with equal exchange couplings on the rungs and legs the interaction between two hole pairs is long ranged and repulsive but becomes attractive and of nearest neighbor type when the strong coupling regime is approached. The same holds for the interaction of a hole pair with the boundaries. We choose a simple form for the interaction between the bosons in order to use only a few parameters. The results obtained from the effective model are insensitive to the specific ansatz used for this interaction. The Luttinger liquid parameter K_ρ has been calculated for electron densities from $\rho = 0.982$ down to $\rho = 0.75$ (half filling corresponds to $\rho = 1$). Down to $\rho \simeq 0.875$ the superconducting correlations are found to be dominant and $K_\rho \to 1$ for $\rho \to 1$. For commensurate filling, $\rho = 0.75$, there might be true charge density wave ordering and a charge gap. Further investigations are necessary to clarify this question. The hopping matrix element for the bosons in the effective model, which allows one to calculate the inverse compressibility, could also be determined. Comparing to the t-J model we find good agreement for strong rung couplings and only small deviation (less than $\pm 10\%$) near the isotropic case.

An interesting feature appeared in the hole-hole correlation function. The correlation length, ξ_{hhc}, does not monotonically increase as one approaches the isotropic case from strong rung coupling. Instead, it decreases in the interval $0.7\,t \leq J' \leq 1.2\,t$. This unexpected behavior can be traced to the fact that the interaction between holes is dominated by the simple rung exchange bonds in the strong rung coupling regime and by the diagonal rung exchange bonds near the isotropic case, $J' \to J$. Reflections of the structure in ξ_{hhc} as a function of J', shown in Fig. 2, can also be found in other properties, e.g. the interaction of the effective bosons with the boundaries and the compressibility.

ACKNOWLEDGMENTS

[1] L. Balents, M. P. A. Fisher, Phys. Rev. B **53**, 12133 (1996)

[2] E. Dagotto, J. Riera and D. Scalapino, Phys. Rev. B **45**, 5744 (1992)

[3] T. M. Rice, S. Gopalan, M. Sigrist, Europhys. Lett. **23**, 445 (1993)

[4] H. Tsunetsugu, M. Troyer, T. M. Rice, Phys. Rev. B **49**, 16078 (1994)

[5] M. Troyer, H. Tsunetsugu, T. M. Rice, Phys. Rev. B **53**, 251 (1996)

[6] E. Dagotto and T. M. Rice, Science **271**, 618 (1996)

[7] F. C. Zhang, T. M. Rice, Phys. Rev. B **37**, 3759 (1988)

[8] S. R. White, Phys. Rev. Lett. **69**, 2863 (1992)

[9] I. Peschel, X. Wang, M. Kaulke, K. Hallberg, Density-Matrix Renormalization - A New Numerical Method in Physics, Springer, ISBN: 3-540-66129-8

[10] S. R. White and D. J. Scalapino, Phys. Rev. B **55**, 6504 (1997)

[11] A. Luther and I. Peschel, Phys. Rev. B **12**, 3908 (1975)

[12] H. D. M. Haldane, Phys. Rev. Lett. **45**, 1358 (1980)

[13] H. J. Schulz, Phys. Rev. Lett. **64**, 2831 (1990)

[14] H. J. Schulz, Phys. Rev. B. **59**, R2471 (1999)

[15] C. A. Hayward, D. Poilblanc, R. M. Noack, D. J. Scalapino, W. Hanke Phys. Rev. Lett. **75**, 926 (1995)

[16] C. A. Hayward, D. Poilblanc, Phys. Rev. B. **53**, 11721 (1995)
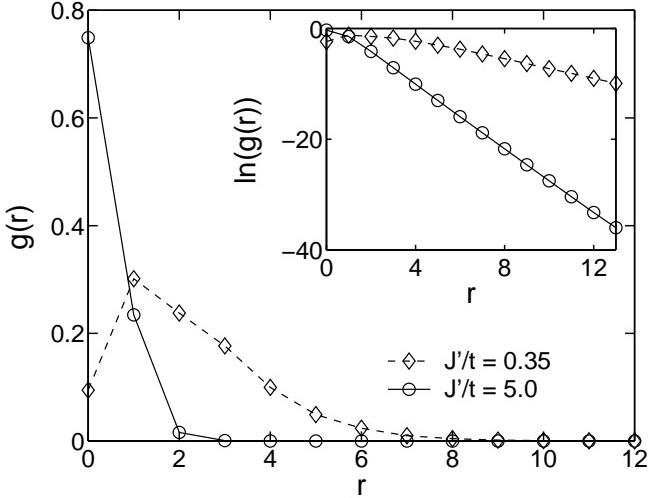
FIG. 1. Hole-hole-correlation function $g(r)$ obtained from DMRG calculations on a (40×2) t-J ladder for $J' = 0.35\,t$ and $J' = 5.0\,t$ with one hole pair ($J = 0.35\,t$, $t = t'$).


FIG. 3. Exchange bonds $\langle \mathbf{S}_i \cdot \mathbf{S}_j \rangle$ around two dynamic holes after projection: $t = t'$, $J = 0.35\,t$, $J' = 1.2\,t$ for the upper and $J = 0.35\,t$, $J' = 0.70\,t$ for the lower figure. The thickness of the lines is proportional to the bond strength.

TABLE I. Parameters for the interaction potential V_{int} given in Eq. (16) obtained from the density profiles of a (30×2) t-J ladder for various J' ($J = 0.35\,t$, $t = t'$).

J'	r_{min}	v_1	v	ξ
0.35	2	4.973	0.478	0.376
0.5	$\frac{3}{2}$	1.28	0.580	0.373
1.	1	10.99	0.586	0.439
2.	1	5.00	0.089	0.363
5.	1	-0.048	0.0029	0.400
10.	1	-0.13	0.0	-
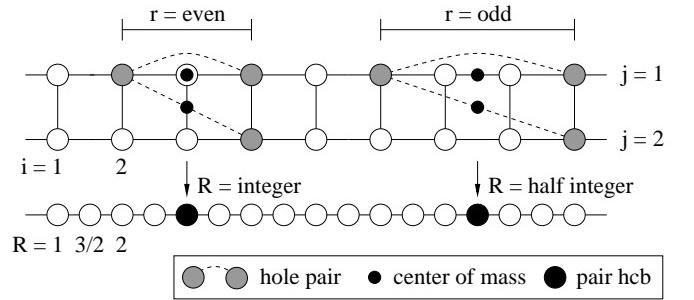
FIG. 4. Mapping of pairs of holes from a ladder to hcb on a chain depending on the different positions of their center of mass and their relative separation r along the legs. R denotes the center of mass coordinate along the legs.

FIG. 2. Correlation length ξ_{hhc} of the hhc-function $g(r)$ as a function of J' ($J = 0.35\,t$, $t = t'$) measured on a (40×2) t-J ladder.
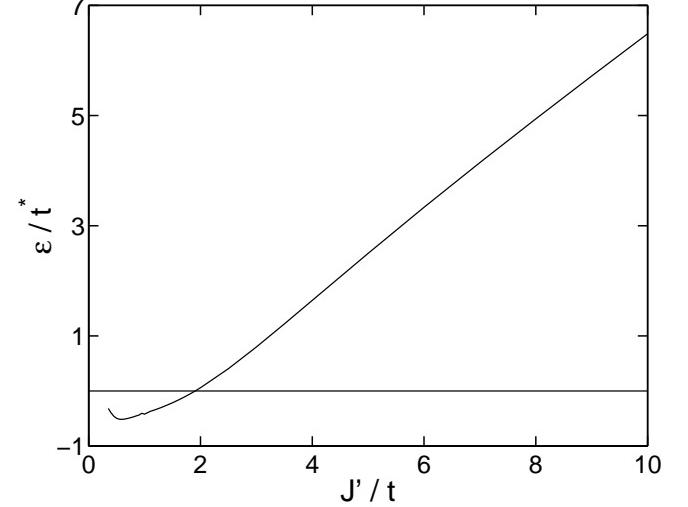
FIG. 5. The onsite potential ϵ obtained from Eq. (11) as a function of J' ($J = 0.35\,t$, $t = t'$). The hhc-functions were obtained from DMRG calculations on (40×2) t-J ladders.
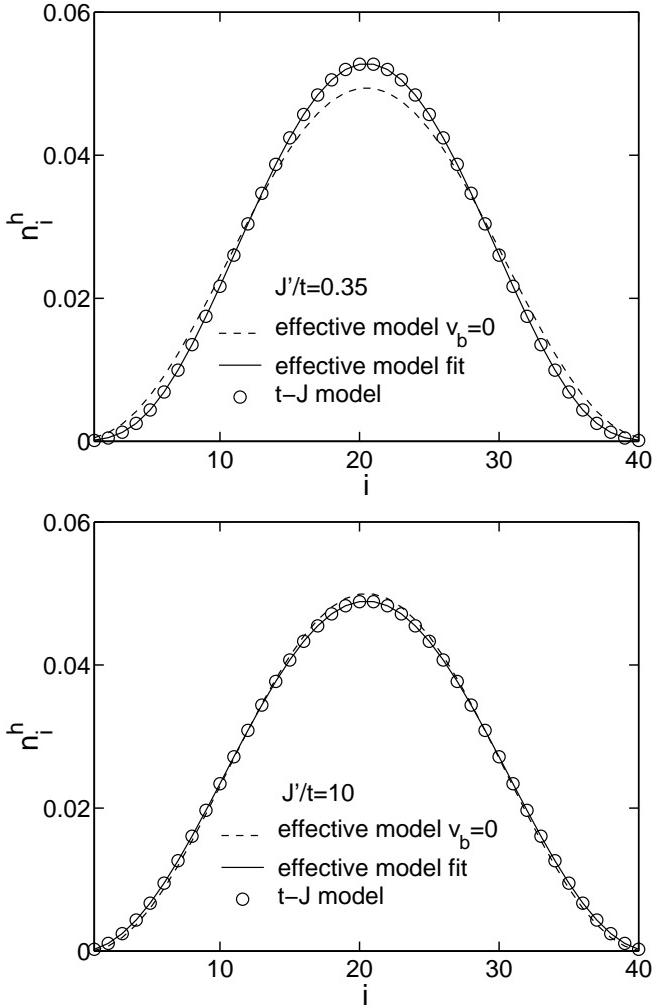
FIG. 6. Hole density n_i^h for two holes on a (40×2) t-J ladder with $J' = 0.35\,t$ and $J' = 10\,t$ $(J = 0.35\,t,\ t = t')$ computed directly and with the effective model. For the effective model the data for $v_b = 0$ and the best fit is shown.
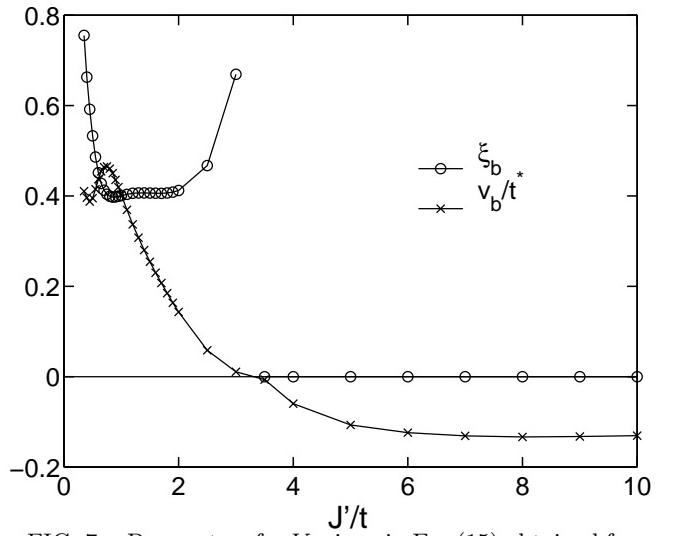

FIG. 7. Parameters for V_b given in Eq. (15) obtained from fits with (40×2) t-J ladders with one hole pair $(J = 0.35\,t,$ $t = t')$.
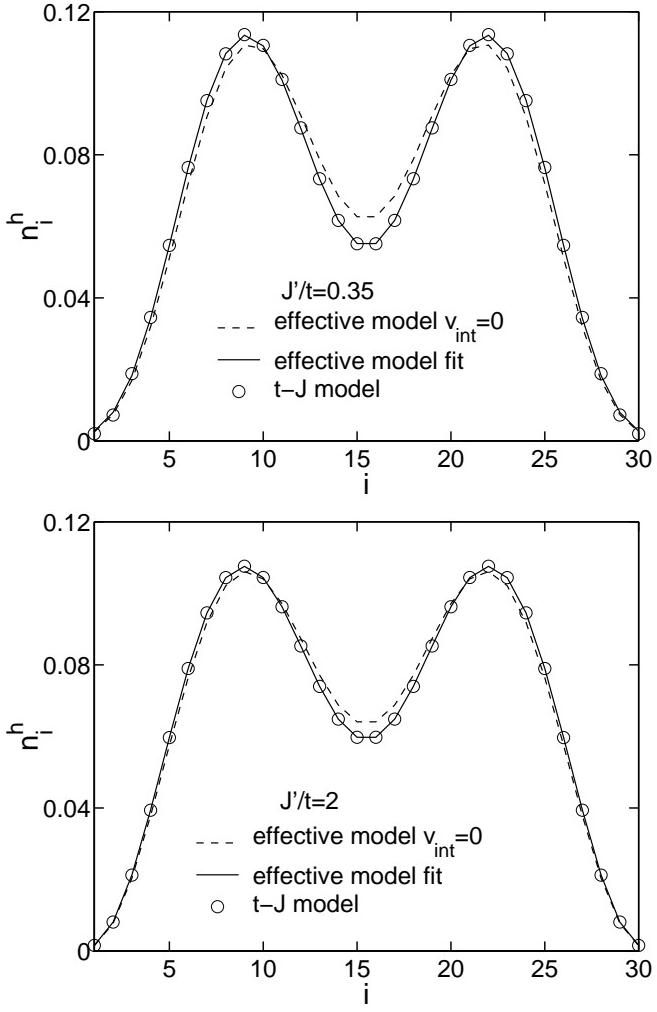
FIG. 8. Hole density n_i^h for $J' = 0.35\,t$ and $J' = 2\,t$ calculated for four holes on a (30×2) t-J ladder computed directly and with the effective model ($J = 0.35\,t$, $t = t'$). For the effective model the data for $v_{\text{int}} = 0$ and the best fit is shown.
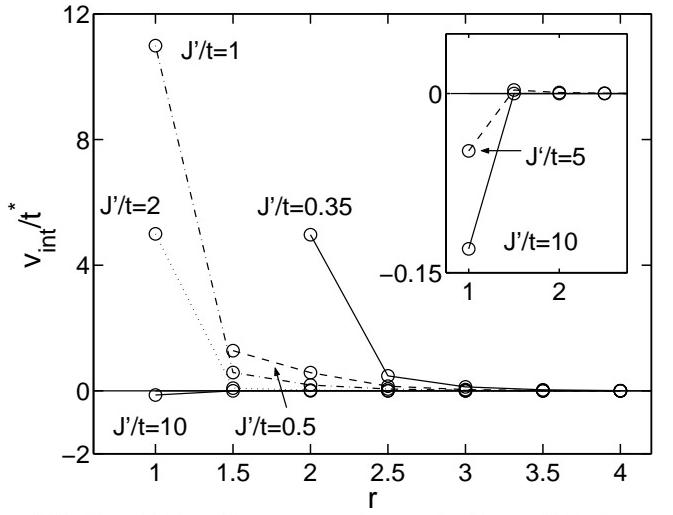
FIG. 9. Interaction parameter $v_{\text{int}}(r \geq r_{\min})$ between the hcb obtained from (30×2) t-J ladders for various J' ($J = 0.35\,t$, $t = t'$).
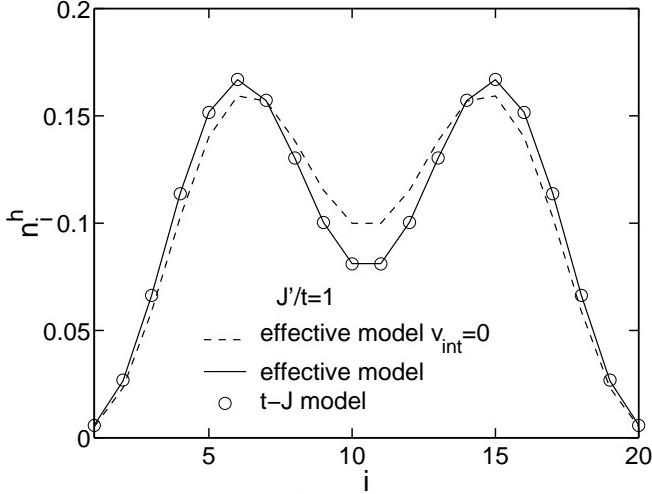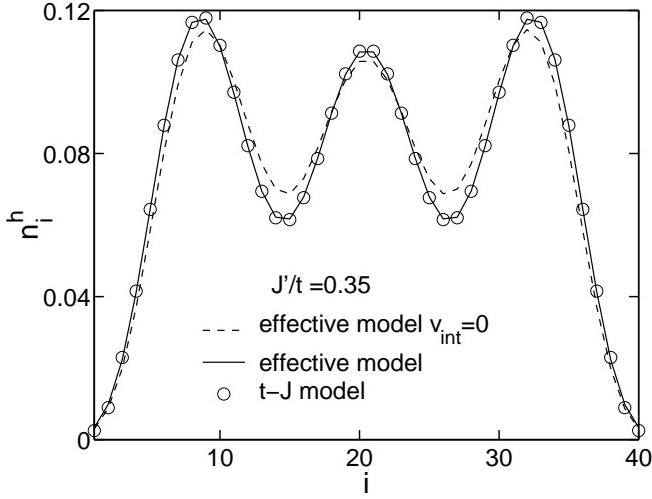
FIG. 10. Hole density n_i^h for $J' = 0.35\,t$ and $J' = t$ for six holes on (40×2) and four holes on (20×2) sites respectively, computedwith the interaction potentials obtained from fits with two hole-pairs on 30 sites ($J = 0.35\,t$, $t = t'$). For the effective model the data for $V_{\mathrm{int}} = 0$ is also shown.
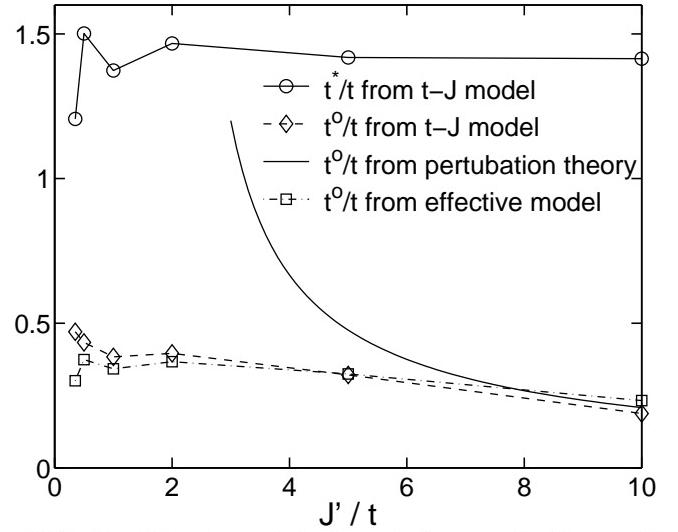
FIG. 11. Hopping matrix elements for our effective model and for the model in Ref. [5] obtained for the large J' limit ($J = 0.35\,t$, $t = t'$). Explanations are in the text.
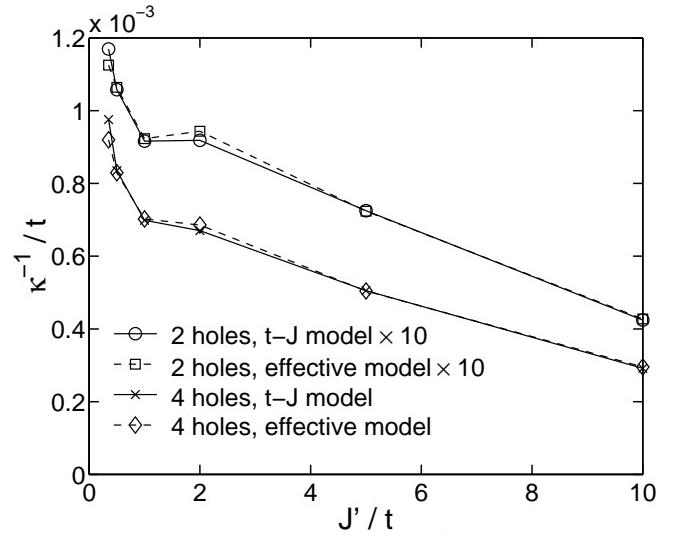
FIG. 12. Inverse compressibility κ^{-1} for the t-J Ladder computed directly and with the corresponding effective model for 2 holes (magnified $10\times$) and 4 holes for a 40×2 t-J ladder ($J = 0.35\,t$, $t = t'$).
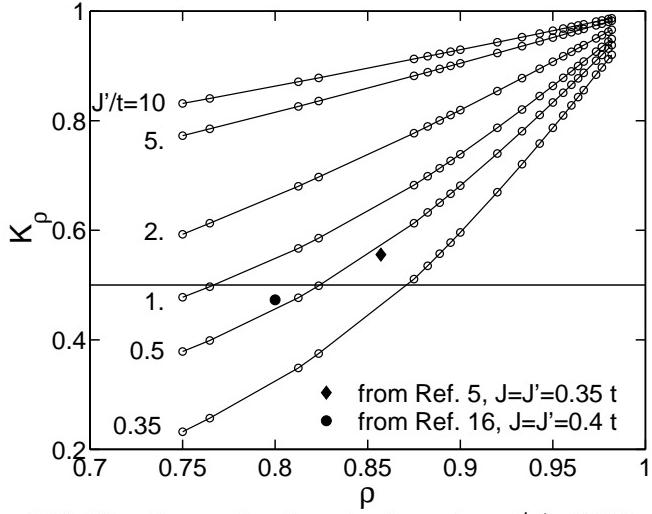
FIG. 13. K_ρ as a function of ρ for various J' (half filling is given by $\rho = 1$, $J = 0.35\,t$, $t = t'$).


FIG. 15. Density profile n_i^h computed with the effective model for a (200×2) t-J ladder at one quarter doping ($\rho = 0.75$) with the parameters of the isotropic case ($J = J' = 0.35\,t$, $t = t'$), showing a pinned CDW.


FIG. 14. K_ρ as a function of J' for various electron densities ρ (half filling is given by $\rho = 1$, $J = 0.35\,t$, $t = t'$).
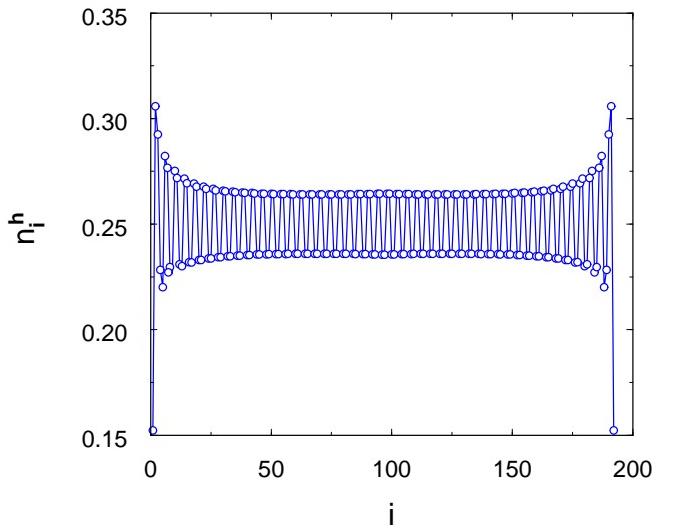
FIG. 16. Hole density for a (192×2) t-J ladder at one quarter doping ($\rho = 0.75$) showing a pinned CDW. Here $J' = J = 0.3\,t$ and $t' = t$.